NANO LETTERS

2002
Vol. 2, No. 3
187−190

Scanned Conductance Microscopy of Carbon Nanotubes and λ-DNA

Marc Bockrath,* Nina Markovic, Adam Shepard, and M. Tinkham

Department of Physics, Harvard University, 9 Oxford Street, Cambridge, Massachusetts 02138

Leonid Gurevich and Leo P. Kouwenhoven

Department of Applied Physics and DIMES, Delft University of Technology, P.O. Box 5046, 2600 GA Delft, The Netherlands

Mingshaw W. Wu and L. L. Sohn

Department of Physics, Princeton University, Princeton, New Jersey 08544

Received September 25, 2001; Revised Manuscript Received November 27, 2001

ABSTRACT

We have devised a scanned probe technique based on electrostatic force microscopy capable of probing the conductance of samples without requiring attached leads. We demonstrate that, using our technique, conductance can be probed on length scales as small as 0.4 μm. To demonstrate the utility of our technique, we use it to probe the conductance of DNA, a subject that has been the focus of intense debate with reported results ranging from metallic to insulating. In contrast to conducting single-wall carbon nanotubes, used as a control, individual strands of λ-DNA, a widely studied sequence, are found to be insulating on the length scale probed.

Electrostatic force microscopy[1−3] (EFM) is a powerful tool to image electric fields. For example, among its many diverse applications, it has been employed to image potentials in carbon nanotube circuits[4,5] and study ferroelectricity.[6] Here we report a technique based on EFM to image a sample's conductivity on a microscopic scale. We demonstrate that using our technique, conductance can be probed on length scales as small as 0.4 μm, and we believe that with optimization of the sample geometry, this length scale can be reduced yet further. As an illustration, we employ it to investigate the electrical properties of single-walled carbon nanotubes (SWNTs), which are widely studied conducting wires, and DNA, which has been the focus of heated debate concerning its conductance.[7−14] We find that unlike metallic and semiconducting SWNTs, λ-DNA is an electrical insulator with a one-dimensional conductivity less than $\sim 10^{-16}\ \Omega^{-1}$ cm.

The principle of our scanned probe technique is illustrated in the upper inset of Figure 1. A voltage $V_t \sim 2-8$ V is applied to the tip of a Si atomic force microscope (AFM) cantilever. The cantilever is mechanically driven at a frequency f near its resonant frequency f_0 and scanned at a height h above a grounded, oxidized, degenerately doped Si wafer upon which the material under study is placed. This is accomplished by using the lift-mode feature of our AFM [Digital Instruments Nanoscope III], which makes one pass in tapping mode for each line to acquire the topography and then retraces the same line again, using the topographic information to fly above the sample with a constant tip−sample separation. While scanning the sample in the lift-mode pass, the force gradient sensed by the tip changes the effective spring constant of the cantilever, modulating f_0. As the phase lag ϕ between the drive and the cantilever oscillation is approximately linear in frequency near f_0, this f_0 modulation can be imaged by producing a gray scale plot of ϕ as a function of tip position. A typical result for individual SWNTs[15] on a Si wafer capped with 1 μm of SiO_2 is shown in the main panel of Figure 1, which shows a uniform white background with dark lines, indicating shifts in ϕ. Comparison of these phase images with simultaneously acquired topographic images shows that the dark lines occur whenever the tip is over a nanotube. Inspection of the main panel of Figure 1 reveals that shorter tubes appear relatively fainter than longer tubes. Indeed, nanotubes shorter than $L_{min} \sim 0.4$ μm are not discernible in the phase images.

This behavior can be understood by considering the cantilever tip, nanotube, and the degenerately doped Si as capacitor elements. The voltage applied between the tip and the doped Si produces electrostatic forces on the tip that alter f_0 and ϕ. When the tip is far from a tube, these electrostatic forces are independent of horizontal displacements of the

10.1021/nl0100724 CCC: $22.00
Published on Web 02/07/2002

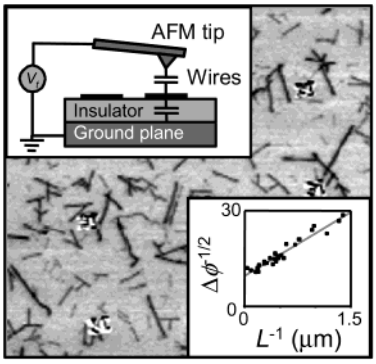

Figure 1. (Upper inset) experimental setup. An AFM cantilever is driven near its resonant frequency. The tip is scanned over a grounded oxidized Si wafer with the samples under study on its surface. After acquiring topography for each line, the tip is retracted by ~30 nm and the line retraced to obtain the electrostatic force data. A scanned conductance image is obtained by producing a gray scale plot of the phase lag ϕ between the cantilever drive and oscillation as a function of tip position. (Main panel) scanned conductance image for single-wall carbon nanotubes. Dark lines indicate shifts in ϕ relative to the background value ϕ_0 occurring whenever the tip is over a tube. The ~1 μm square features are evaporated Au alignment marks. (Lower inset) plot of $(\Delta\phi)^{-1/2} = (\phi - \phi_0)^{-1/2}$ vs the inverse tube length L^{-1} for 26 individual tubes. The data follow a straight line.

tip. The phase ϕ thus takes on a position-independent background value ϕ_0.[16] When the tip is over a tube, the tip-induced charge modulation within the tube produces additional electrostatic tip−sample forces. In this case, the magnitude of these forces and hence ϕ is determined by the electric field between the tip and tube, which in turn depends on the division of V_t between the tip-tube capacitor and the tube−ground−plane capacitor. Because shorter tubes have less capacitance to the ground plane, their potential floats nearer to V_t, yielding smaller tip−tube voltages and smaller phase shifts, as observed.

This can be placed on a quantitative basis by considering the division of V_t between the tip−tube capacitor C_{tt} and tube−ground−plane capacitor C_0L, where C_0 is the capacitance per unit length of the tubes and L is the tube length. Using the elementary result for a capacitive voltage divider, the tip−tube voltage V_{tt} is given by

$$V_{tt} = V_t \frac{C_0 L}{C_0 L + C_{tt}} \tag{1}$$

Furthermore, treating the cantilever as a harmonic oscillator and considering the addition of the electrostatic energy $^1/_2 C_{tt} V_{tt}^2$ to its mechanical energy yields the result that

$$(\phi - \phi_0) \cong \frac{Q}{2k}\frac{d^2 C_{tt}}{dz^2} V_{tt}^{\ 2} = \frac{Q}{2k}\frac{d^2 C_{tt}}{dz^2} V_t^2 \left(\frac{C_0}{C_0 + L^{-1} C_{tt}}\right)^2 \tag{2}$$

where $Q \sim 250$ is the cantilever quality factor, $k \sim 40$ N/m is the spring constant, z is the vertical deflection of the cantilever, and the phase angles are measured in radians. Rearranging eq 2 gives

$$(\phi - \phi_0)^{-1/2} = a + bL^{-1}$$

$$a = \left(\frac{Q}{2k}\frac{d^2 C_{tt}}{dz^2}\right)^{-1/2} V_t^{-1} \qquad b = a\frac{C_{tt}}{C_0} \tag{3}$$

This indicates that plotting $(\phi - \phi_0)^{-1/2}$ vs L^{-1} for tubes of different lengths should yield a straight line. We find that this is indeed the case, as shown in the lower inset to Figure 1, where the measured data follows a straight line with slope $b = 13.6\ \mu m^{-1}$ and an intercept $a = 9.5$.

As is evident from this linear behavior, $(\phi - \phi_0)^{-1/2}$ becomes progressively larger as L^{-1} increases, or alternatively $(\phi - \phi_0)$ decreases as L becomes smaller. This quantifies our observation that shorter wires lead to fainter features in the phase image. For sufficiently short wires, the phase shift should fall below the noise level $\delta\phi_N \sim 10^{-3}$ present in our experiment. Extrapolating the best fit straight line to our data to the limit $(\phi - \phi_0)^{-1/2} = \delta\phi_N^{-1/2} \sim 32$ indicates that $(\phi - \phi_0) = \delta\phi_N$ when $L = L_{min} \sim 0.4\ \mu$m, consistent with our previous observation that wires shorter than L_{min} are not discernible in the phase image. We note that we made no effort to optimize the sample geometry to minimize L_{min}, which may be done, for example, by reducing the thickness of the SiO_2 layer to increase C_0.

Having addressed the minimum length of a detectible conducting wire, we now determine its minimum conductance. A maximal phase shift requires the entire wire to be polarized, taking a characteristic time τ_{RC} equal to the RC time constant of the wire, while the tip scans over a wire in a characteristic time τ_{scan}. Thus, the criterion for a detectible wire depends on the comparison of these two time scales; the tip must remain near a tube long enough for complete polarization to occur. For a wire with one-dimensional conductivity G_0, $\tau_{RC} = C_0L^2/G_0$, and comparing τ_{scan} and τ_{RC}, we find $G_0 \geq G_{min} = C_0L^2/\tau_{scan}$ for a fully detectible wire. For $G_0 < G_{min}$, the measured signal should be reduced toward zero.

Obtaining values for G_{min} appropriate for our geometry requires an estimate for C_0. This information is provided by the linear fit shown in the lower inset to Figure 1, which can be used to obtain estimates for both C_{tt} and C_0. Under the conditions of the measurement shown in Figure 1, $h \sim 120$ nm and $V_t = 6$ V, and we find from an order of magnitude estimate based on eq 2 that $C_{tt} \sim 2kh^2/Qa^2V_t^2 \sim 1.4 \times 10^{-18}$ F. Moreover, inspection of eq 2 yields $b/a = C_{tt}/C_0 = 1.4$, which gives $C_0 \sim 2.0 \times 10^{-18}$ F/μm. This value for C_0 can be compared to an a priori estimate treating the nanotubes as wires of radius $r \sim 1$ nm that are a distance $d = 1\ \mu$m above a parallel conducting plane, which yields $C_0 \sim 2\pi\epsilon_0/\ln(2d/r) = 7 \times 10^{-18}$ F/μm, in reasonable agreement with the estimate obtained directly from our measurements.

Using these estimates for C_0, we present a summary of the length and conductance limits to detectible wires in the graph shown in Figure 2. Each point on the graph represents a wire of length L and conductance G_0. The dashed line is the boundary set by the conductance limit using $C_0 = 10^{-17}$ F/μm, taken as a representative value, and $\tau_{scan} = 10^{-3}$ s. The solid line is the boundary set by L_{min}. The hatched area

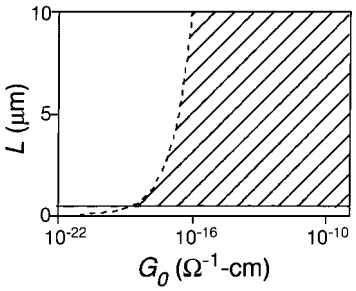

Figure 2. Graph depicting the combinations of wire length and conductivity that are detectible via scanned conductance microscopy. The hatched region corresponds to detectible wires. The dashed line is the limit set by the conductivity, while the solid line is the limit set by the length, as discussed in the text.

indicates combinations of L and G_0 that produce detectible wires. For wires far to the left of the dashed line, the measured phase signal should tend toward zero and eventually fall beneath $\delta\phi_N$. Whether wires with parameter values in this region are detectible or not thus depends on a consideration of the signal-to-noise ratio, and hence the determination of the precise boundary between detectible and nondetectible wires requires more detailed calculations. Nevertheless, the hatched region shown in Figure 2 can be taken to give a reasonable approximation to combinations of L and G_0 producing detectible wires. For comparison, metallic tubes typically have $G_0 \sim 10^{-8}\ \Omega^{-1}$ cm, while semiconducting tubes typically have $G_0 \sim 10^{-11}\ \Omega^{-1}$ cm.[17] As these values fall well to the right of the dashed line in Figure 2, it is not surprising that all SWNTs exceeding L_{min} appear in this scanned conductance (SC) image.[18] The AFM tip essentially acts as a "metal detector" capable of detecting extraordinarily low conductivity wires.

We exploit this capability to investigate the electrical properties of λ-DNA. After placing SWNTs on a chip with predefined alignment marks, λ-DNA is added to the surface from a drop of λ-DNA in a pH 8, 10 mM Tris−HCl, 1 mM EDTA solution, which is then blown dry with nitrogen gas, rinsed with a pH 6.1, 20 mM solution of ammonium acetate, and blown dry again. We distinguish the λ-DNA from the nanotubes, which are similar in diameter and length to the λ-DNA and serve as a control for this experiment, in one of two ways. In the first method, the SWNTs are located relative to the alignment marks prior to depositing the DNA. Strands that did not appear previously are taken to be λ-DNA. In the second method, following our experiments, the λ-DNA is removed from the sample by treating the wafer with DNA AWAY [Molecular BioProducts], a commercially available cleaning agent used to specifically remove DNA. With the λ-DNA removed, an ex post facto assignment of the remaining wires as being SWNTs is then made, allowing the two types of wire to be distinguished in our data. In the data discussed below, we employ the second method.

A colorized topographic image with both SWNTs and λ-DNA is shown in Figure 3a, with the λ-DNA shown in green, the SWNTs shown in red, and a 1 μm gold alignment mark shown in yellow. To exhibit this topographic data more quantitatively, Figure 3b shows a gray scale plot of the

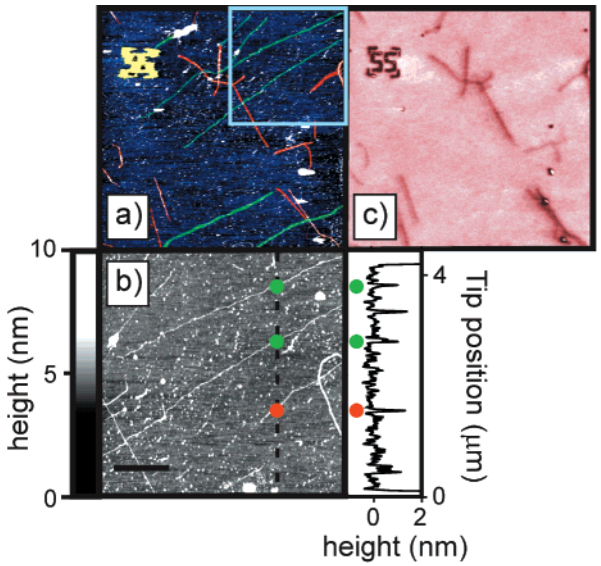

Figure 3. (a) Colorized topographic image of SWNT bundles and single tubes, colored red, and λ-DNA molecules, colored green. A 1 μm alignment mark is shown in yellow. (b) 4.5 μm × 4.5 μm topographic scan of the region enclosed by the blue square in Figure 3a. The higher resolution scan shows the topographic features more clearly than is possible with the larger area scan in part (a). The gray level scale is shown to the immediate left of the image. The scale bar is 1 μm. A SWNT is marked by a red dot, while two λ-DNA molecules are marked by green dots. The graph to the immediate right of the panel shows a line trace through the topographic image along the dotted line, with a constant offset height subtracted from the data. The SWNT and λ-DNA molecules both are ∼1 nm in height. (c) Scanned conductance image of the region shown in part (a). Although the SWNT and the λ-DNA are similar in height, they produce dramatically different signals in the SC image; the conducting nanotubes produce a clear signal, while no signal appears when the tip is over the λ-DNA molecules. This demonstrates that λ-DNA is an insulator with an extremely low conductance.

topography for the 4.5 × 4.5 μm^2 area enclosed by the blue square in Figure 3a. The gray scale is indicated to the left of the image, with black corresponding to 0 nm height, and white corresponding to 10 nm height. A SWNT is marked by a red dot, and two λ-DNA molecules are marked by green dots. The height of the SWNT and λ-DNA is shown in the graph to the right of the image, which shows a line trace taken through the dotted line, with a constant offset height subtracted. Both the λ-DNA molecules and the SWNT are ∼1 nm in height.

Figure 3c shows the scanned conductance (SC) image corresponding to the region shown in Figure 3a. Although the SWNT and λ-DNA molecules are both ∼1 nm in height, they give dramatically different responses in the SC image. Indeed, comparing Figure 3a with Figure 3c reveals that the conducting nanotubes and nanotube ropes yield a clear signal in the SC image, in contrast to the λ-DNA molecules, which yield no signal. We have observed this behavior in a large number of samples (∼20 λ-DNA molecules over 4 different wafers), indicating that on length scales greater than L_{min}, λ-DNA is an electrical insulator with an extremely low conductivity, consistent with the findings of refs 8, 12, and 14.

We expect that our technique will have wide applications toward investigating the electrical properties of materials. For example, we note that although λ-DNA is apparently an electrical insulator, the possibility exists that chemically modified DNA[14] or DNA based on other sequences may be conducting. Our technique provides a simple method to screen rapidly DNA of any sequence or other materials to find potential conductors. Finally, we note that although we have focused here on wires, we expect that conducting two-dimensional sheets, for example, single ~0.3 nm thick sheets of graphite, should also be detectible. This may be useful for locating such sheets on a substrate for the purpose of attaching electrical leads, which may otherwise be difficult because of their small height.

Acknowledgment. We acknowledge helpful discussions with Hongkun Park, tube material from J. H. Hafner and C. M. Lieber, and the support of ONR grant N00014-96-0108 and NSF grants DMR 0072618 and DMR 980936.

References

(1) Martin, Y.; Abraham, D. W.; Wickramasinghe, H. K. *Appl. Phys. Lett.* **1988**, *52*, 1103.
(2) Schönenberger, C.; Alvarado, S. F. *Phys. Rev. Lett.* **1990**, *65*, 3162.
(3) Stern, J. E.; Terris, B. D.; Mamin, H. J.; Rugar, D. *Appl. Phys. Lett.* **1988**, *53*, 2717.
(4) Bachtold, A.; Fuhrer, M.; Plyasunov, S.; Forero, M.; Anderson, E. H.; Zettl, A.; McEuen, P. L. *Phys. Rev. Lett.* **2000**, *84*, 6082.
(5) de Pablo, P. J.; Gomez-Navarro, C.; Gil, A.; Colchero, J.; Martinez, M. T.; Benito, A. M.; Maser, W. K.; Gomez-Herrero, J.; Baro, A. M. *Appl. Phys. Lett.* **2001**, *79*, 2979.
(6) Ahn, C. H.; Tybell, T.; Antognazza, L.; Char, K.; Hammond, R. H.; Beasley, M. R.; Fischer, Ø.; Triscone, J.-M. *Science* **1997**, *276*, 1100.
(7) Porath, D.; Bezryadin, A.; de Vries, S.; Dekker, C. *Nature* **2000**, *403*, 635.
(8) de Pablo, P. J.; Moreno-Herrero, F.; Colchero, J.; Gomez Herrero, J.; Herrero, P.; Baro, A. M.; Ordejon, P.; Soler, J. M.; Artacho, E. *Phys. Rev. Lett.* **2000**, *85*, 4992.
(9) Fink, H. W.; Schönenberger, C. *Nature* **1999**, *398*, 407.
(10) Kasumov, A. Y.; Kociak, M.; Gueron, S.; Reulet, B.; Volkov, V. T.; Klinov, D. V.; Bouchiat, H. *Science* **2001**, *291*, 280.
(11) Tran, P.; Alavi, B.; Grüner, G. *Phys. Rev. Lett.* **2000**, *85*, 1564.
(12) Braun, E.; Eichen, Y.; Sivan, U.; Ben-Yoseph, G. *Nature* **1998**, *391*, 775.
(13) Okahata, Y.; Kobayashi, T.; Tanaka, K.; Shimomura, M. *J. Am. Chem. Soc.* **1998**, *120*, 6165.
(14) Rakitin, A.; Aich, P.; Papadopoulos, C.; Kobzar, Y.; Vedeneev, A. S.; Lee, J. S.; Xu, J. M. *Phys. Rev. Lett.* **2001**, *86*, 3670.
(15) Individual single-walled nanotubes were grown on the surface by chemical vapor deposition; see, for example, Hafner, J. H.; Cheung, C. L.; Lieber, C. M. *J. Am. Chem. Soc.* **1890**, *121*, 9750. Alternatively, SWNT material purchased from Carbon Nanotechnologies was sonicated in dichloroethane and then nanotubes were placed on the surface by placing a drop of the suspension on the surface.
(16) Other forces, for example, van der Waals forces, may also contribute to ϕ_0. This, however, should not change our basic conclusions.
(17) McEuen, P. L.; Bockrath, M.; Cobden, D. H.; Yoon, Y.-G.; Louie, S. G. *Phys. Rev. Lett.* **1999**, *83*, 5098.
(18) Occasionally, we find nanotubes that produce a noticeably smaller phase shift in the SC image than other nanotubes on the same wafer of similar length. We speculate that these tubes are highly resistive due to the presence of defects, or possibly that they are especially resistive semiconducting nanotubes. More experiments are necessary to clarify this issue.

NL0100724